Human cancer tissues exhibit reduced A-to-I Editing of miRNAs coupled with elevated editing of their targets

Yishay Pinto, Ilana Buchumenski, Erez Y. Levanon and Eli Eisenberg

Supplementary Figures (13)

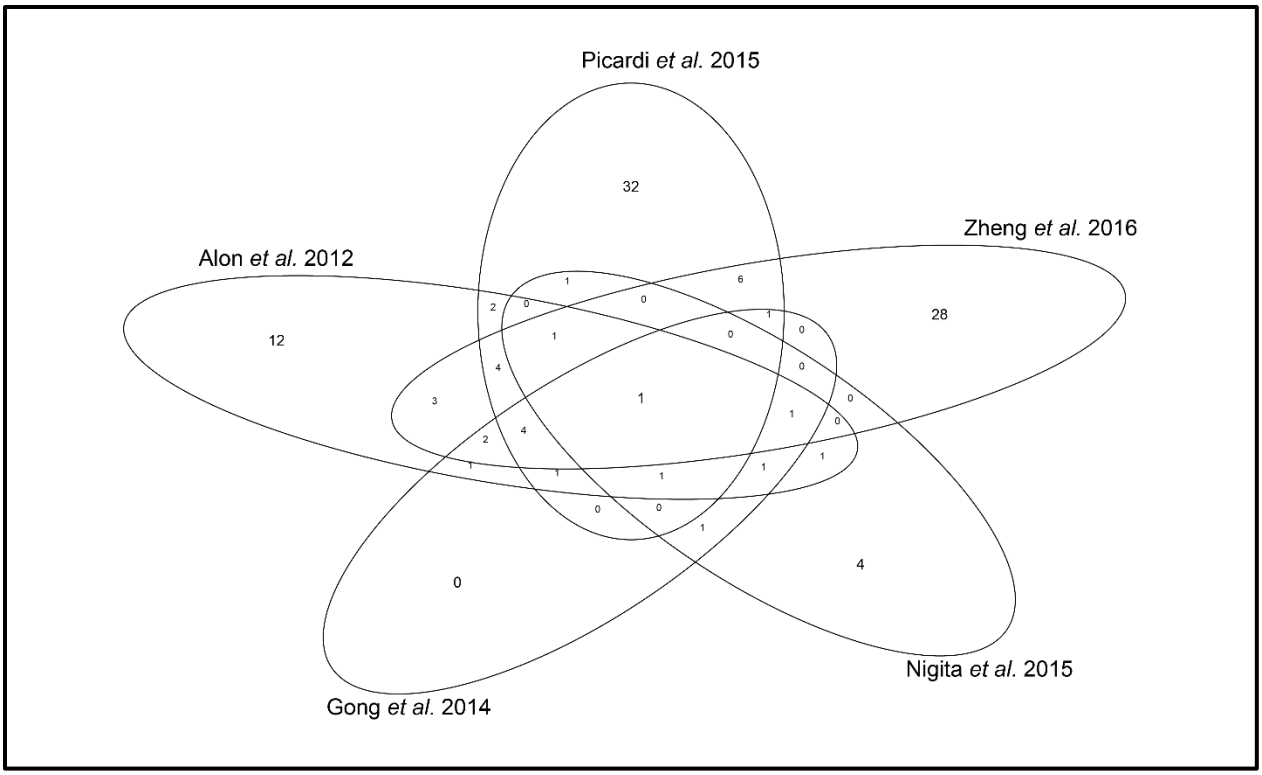

Supplementary Figure S1: Low overlap between different studies that computationally detected de novo A-to-I miRNA editing. Venn diagram of 5 studies that detected miRNA editing sites by analyzing miRNA-seq data.

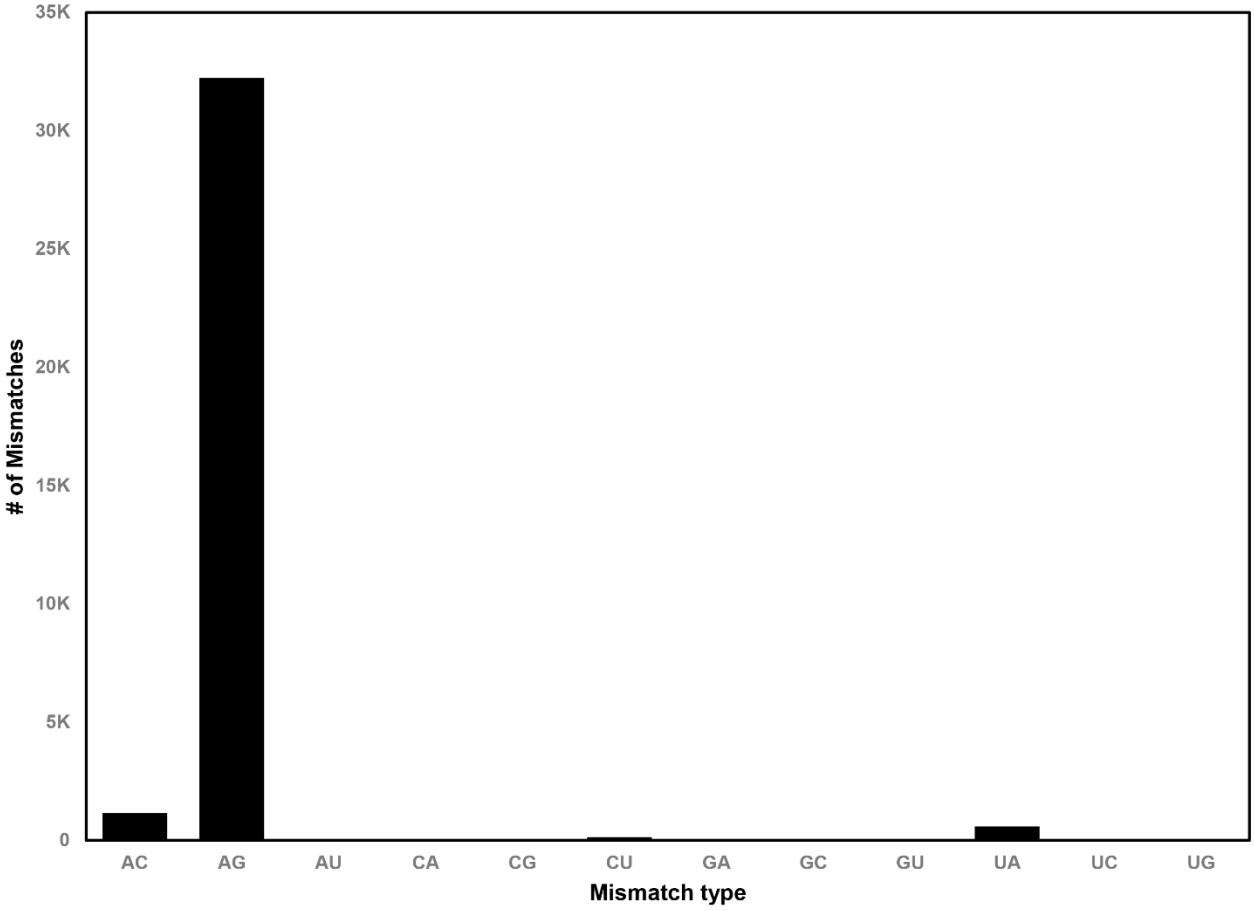

Supplementary Figure S2: De novo mismatches detection shows high enrichment of A-to-G mismatches. Number of mismatches per type following the optimization scheme. Almost only A-to-G mismatches are observed suggesting high signal-to-noise ratio.

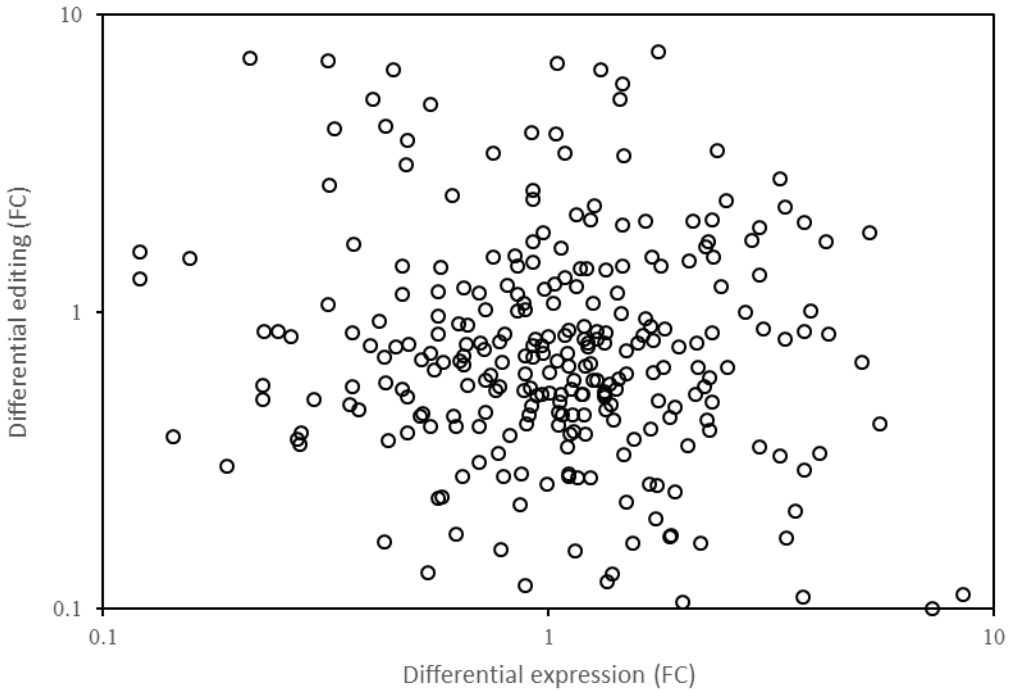

Supplementary Figure S3: Correlation between differential miRNA editing and expression levels. For each of the miRNA with differentially edited site (Figure 3; Supplementary Table S4) we calculated the fold-change (tumor mean/normal mean) of its editing and expression levels and correlated them. No correlation was found (r=-0.02; p=0.69).

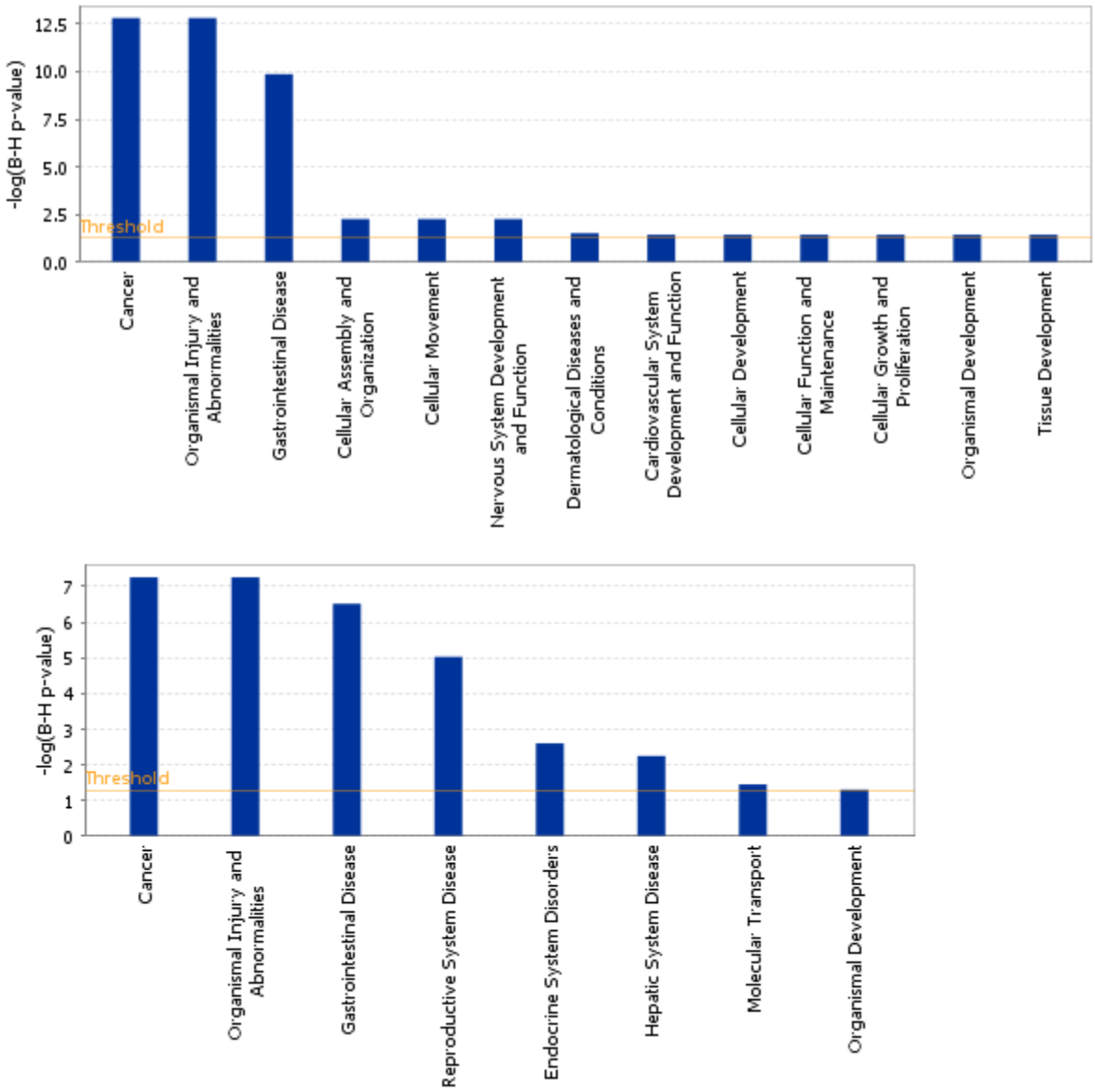

Supplementary Figure S4: Enriched diseases and biological functions for the edited version of miR-376a-5p target genes (upper panel) and for the unedited version of miR-376a-5p target genes (lower panel) by ingenuity pathway analysis (IPA, http://www.ingenuity.com).

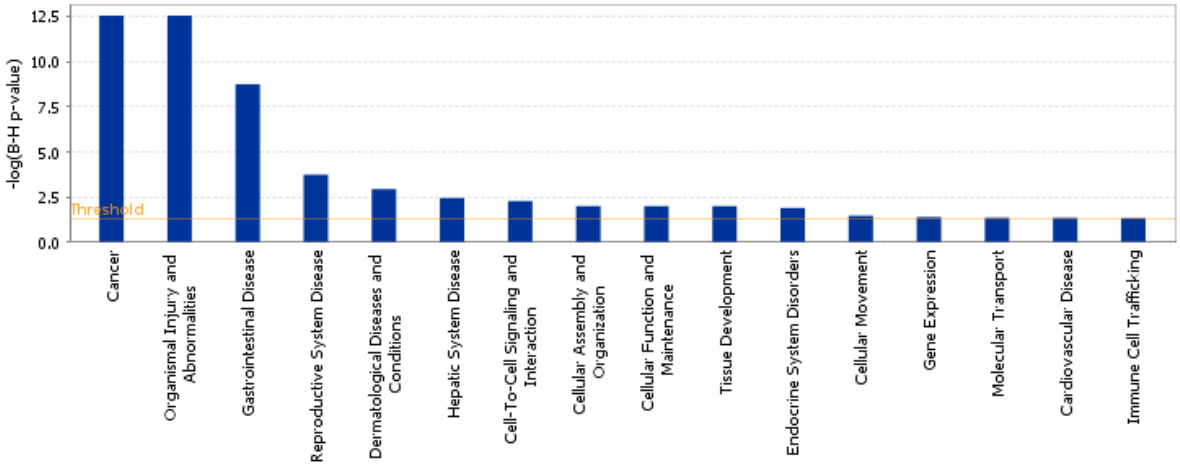

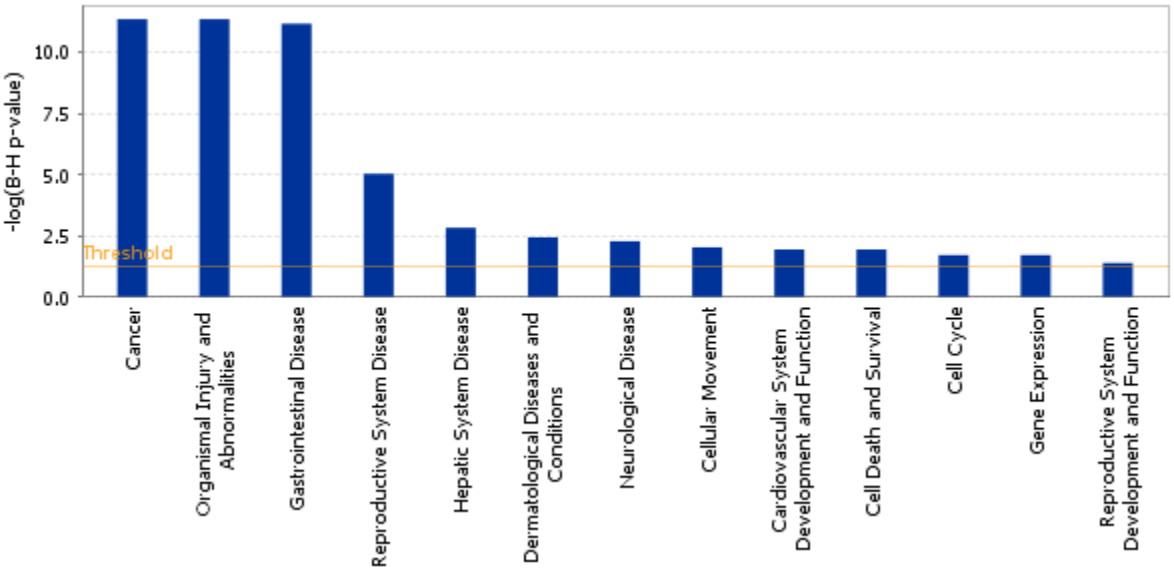

Supplementary Figure S5: Enriched diseases and biological functions for the edited version of miR-376a-3p target genes (upper panel) and for the unedited version of miR-376a-3p target genes (lower panel) by ingenuity pathway analysis (IPA, http://www.ingenuity.com).

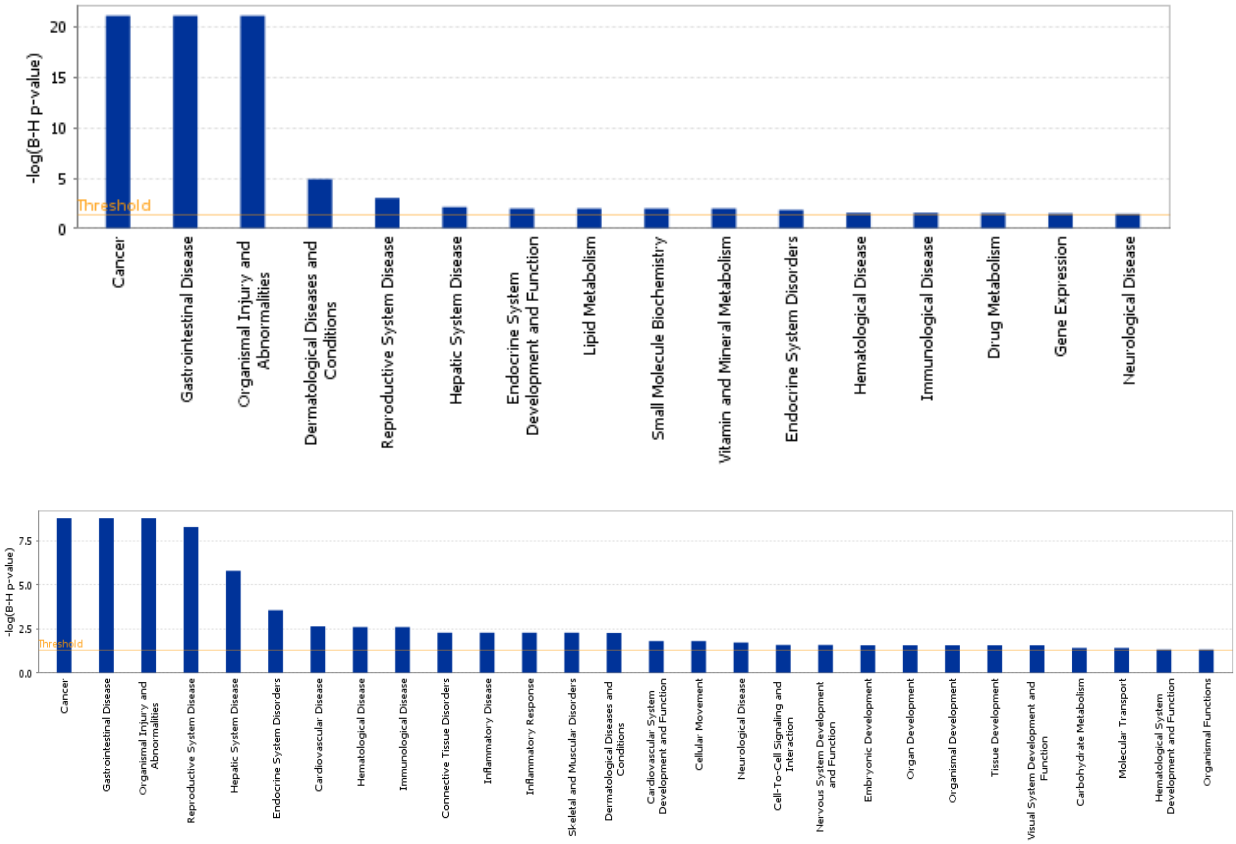

Supplementary Figure S6: Enriched diseases and biological functions for the edited version of miR-376c-3p target genes (upper panel) and for the unedited version of miR-376c-3p target genes (lower panel) by ingenuity pathway analysis (IPA, http://www.ingenuity.com).

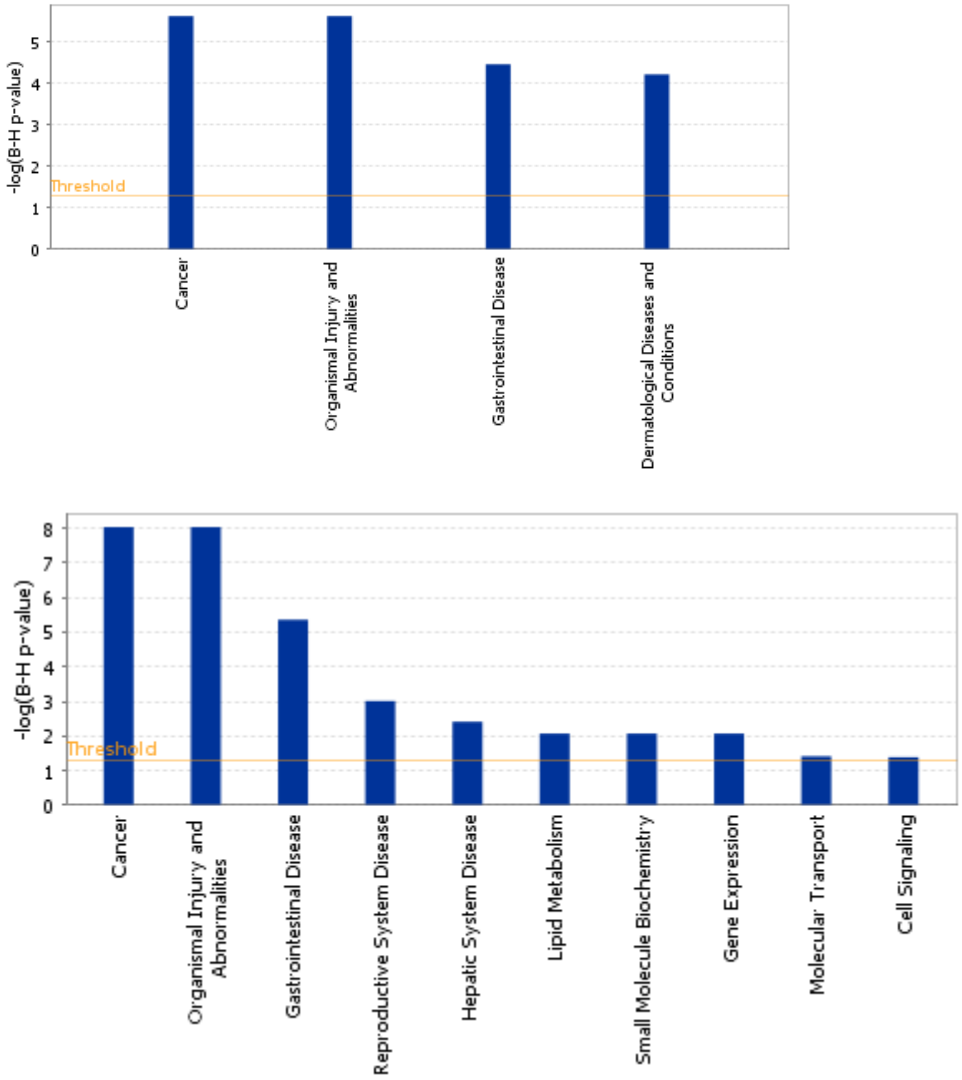

Supplementary Figure S7: Enriched diseases and biological functions for the edited version of miR-381-3p target genes (upper panel) and for the unedited version of miR-381-3p target genes (lower panel) by ingenuity pathway analysis (IPA, http://www.ingenuity.com).

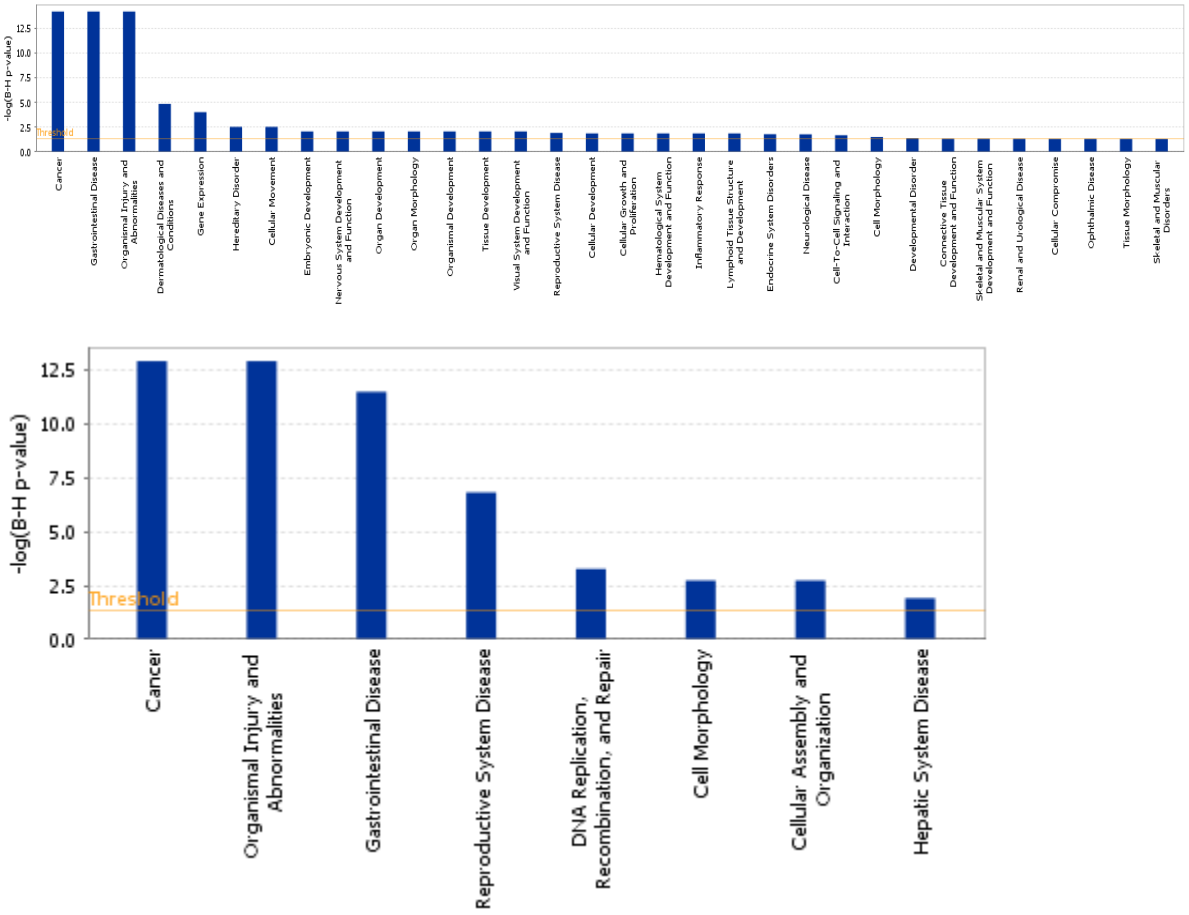

Supplementary Figure S8: Enriched diseases and biological functions for the edited version of miR-411-5p target genes (upper panel) and for the unedited version of miR-411-5p target genes (lower panel) by ingenuity pathway analysis (IPA, http://www.ingenuity.com).

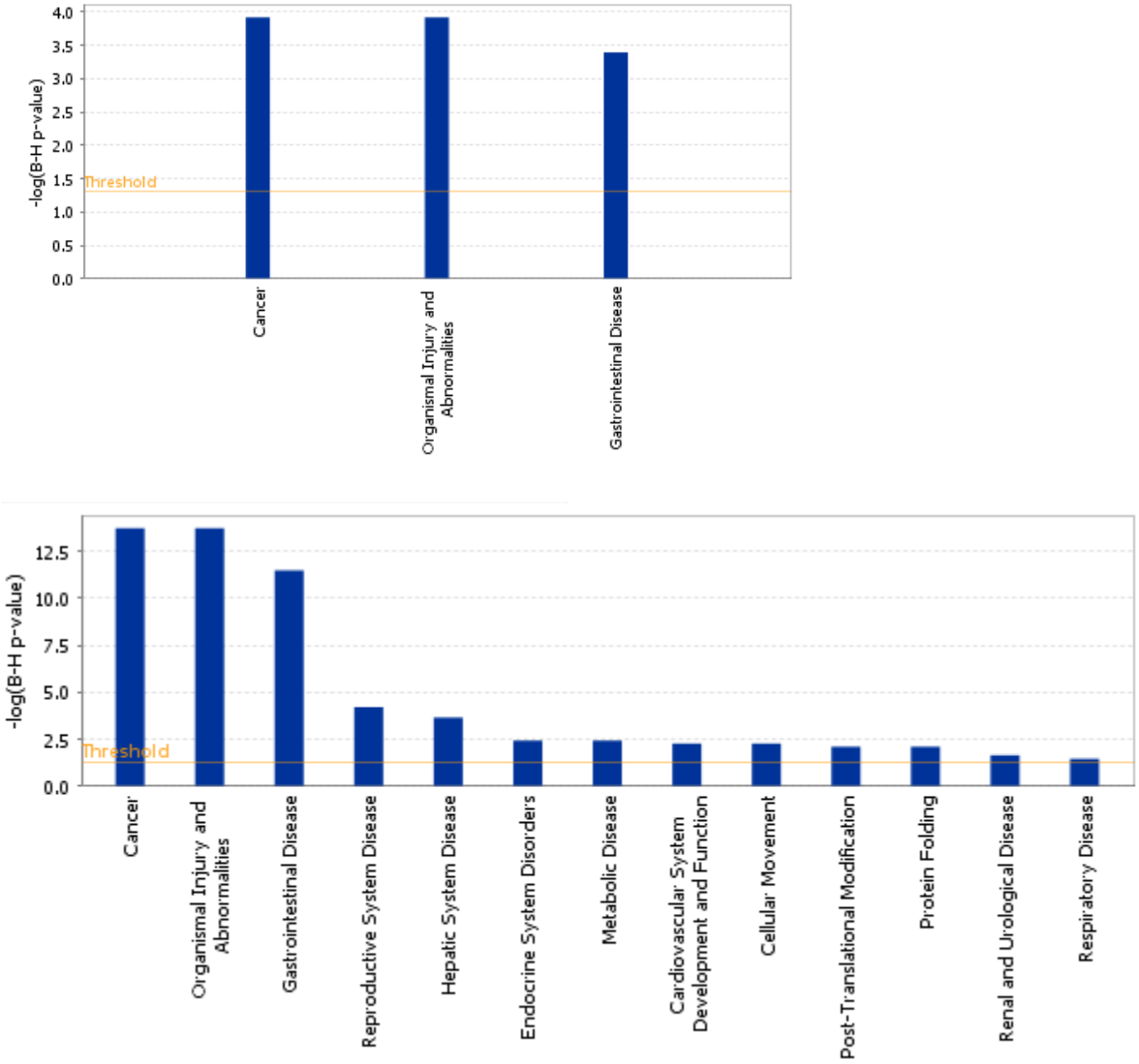

Supplementary Figure S9: Enriched diseases and biological functions for the edited version of miR-497-5p target genes (upper panel) and for the unedited version of miR-497-5p target genes (lower panel) by ingenuity pathway analysis (IPA, http://www.ingenuity.com).

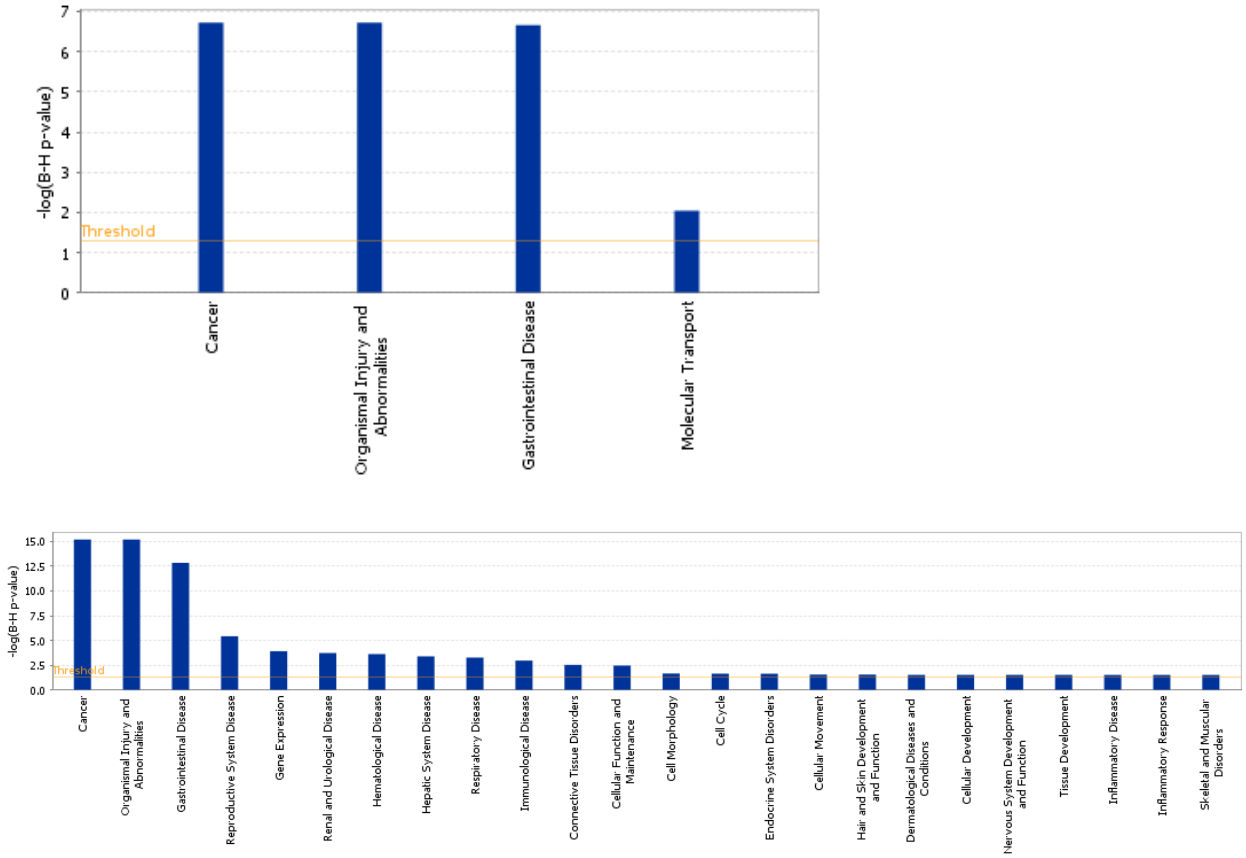

Supplementary Figure S10: Enriched diseases and biological functions for the edited version of miR-589-3p target genes (upper panel) and for the unedited version of miR-589-3p target genes (lower panel) by ingenuity pathway analysis (IPA, http://www.ingenuity.com).

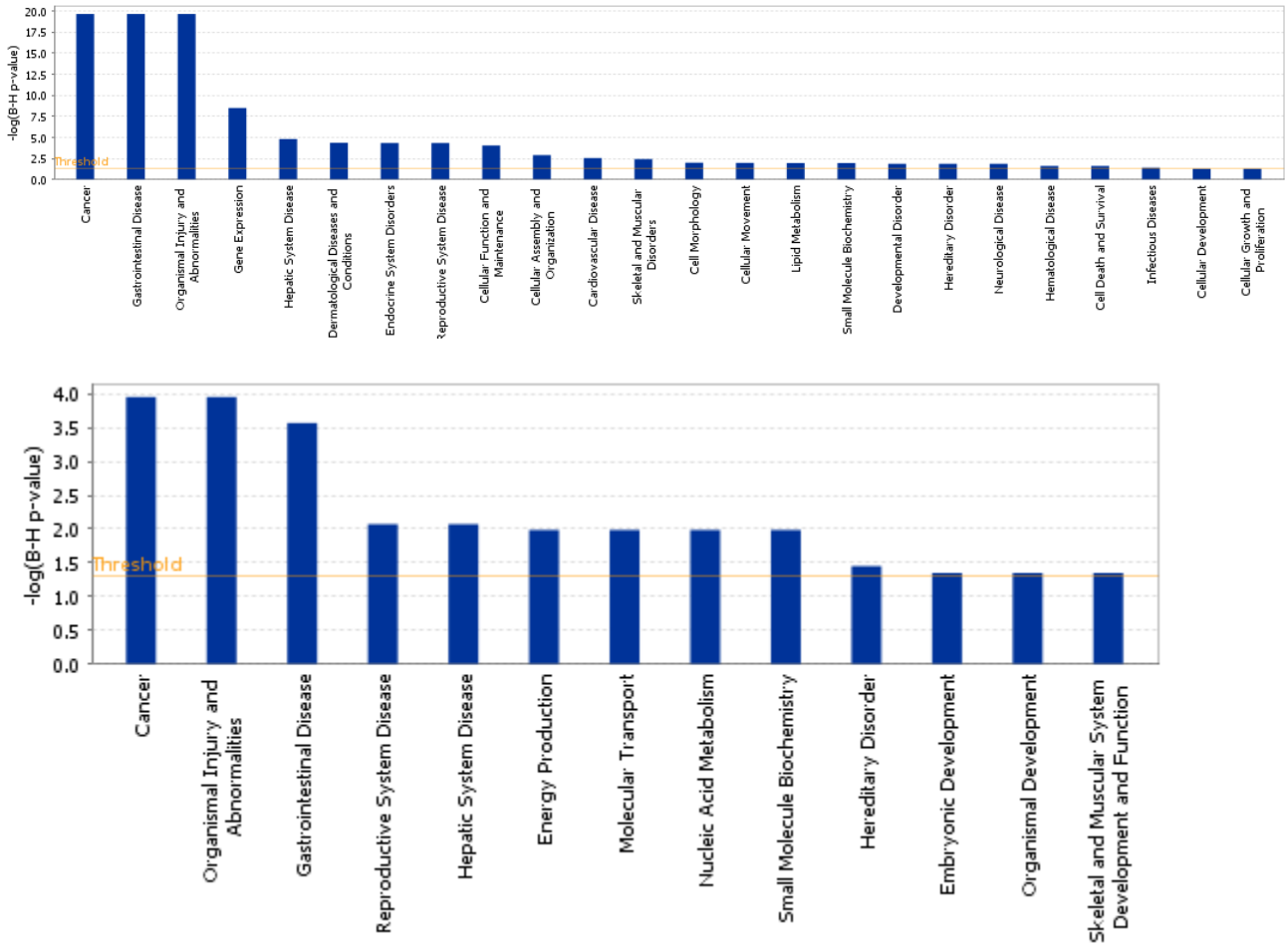

Supplementary Figure S11: Enriched diseases and biological functions for the edited version of miR-6503-3p target genes (upper panel) and for the unedited version of miR-6503-3p target genes (lower panel) by ingenuity pathway analysis (IPA, http://www.ingenuity.com).

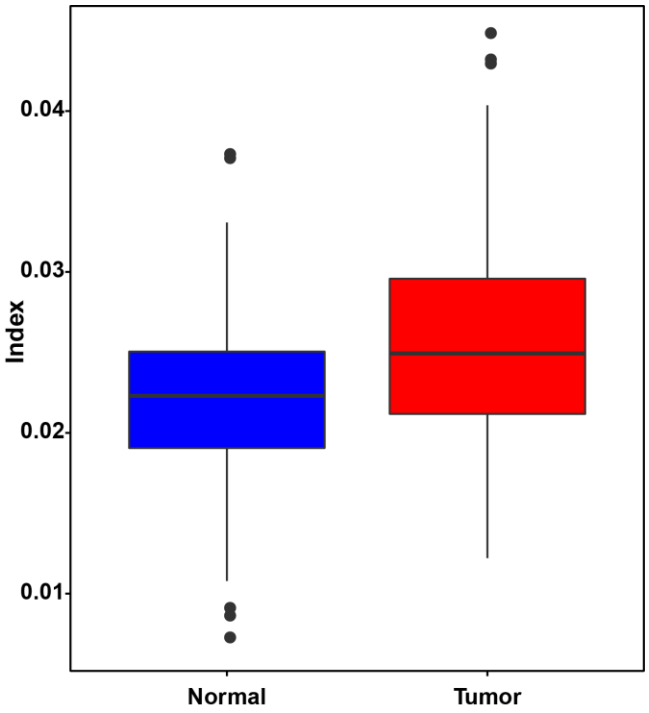

Supplementary Figure S12: Higher global targets-editing levels in tumors in comparison to their matched normal samples. Boxplot of the targets-editing index per sample for all 714 matched samples (Supplementary Table S2). $p=3.55x10^{-22}$, Wilcoxon signed-rank test.

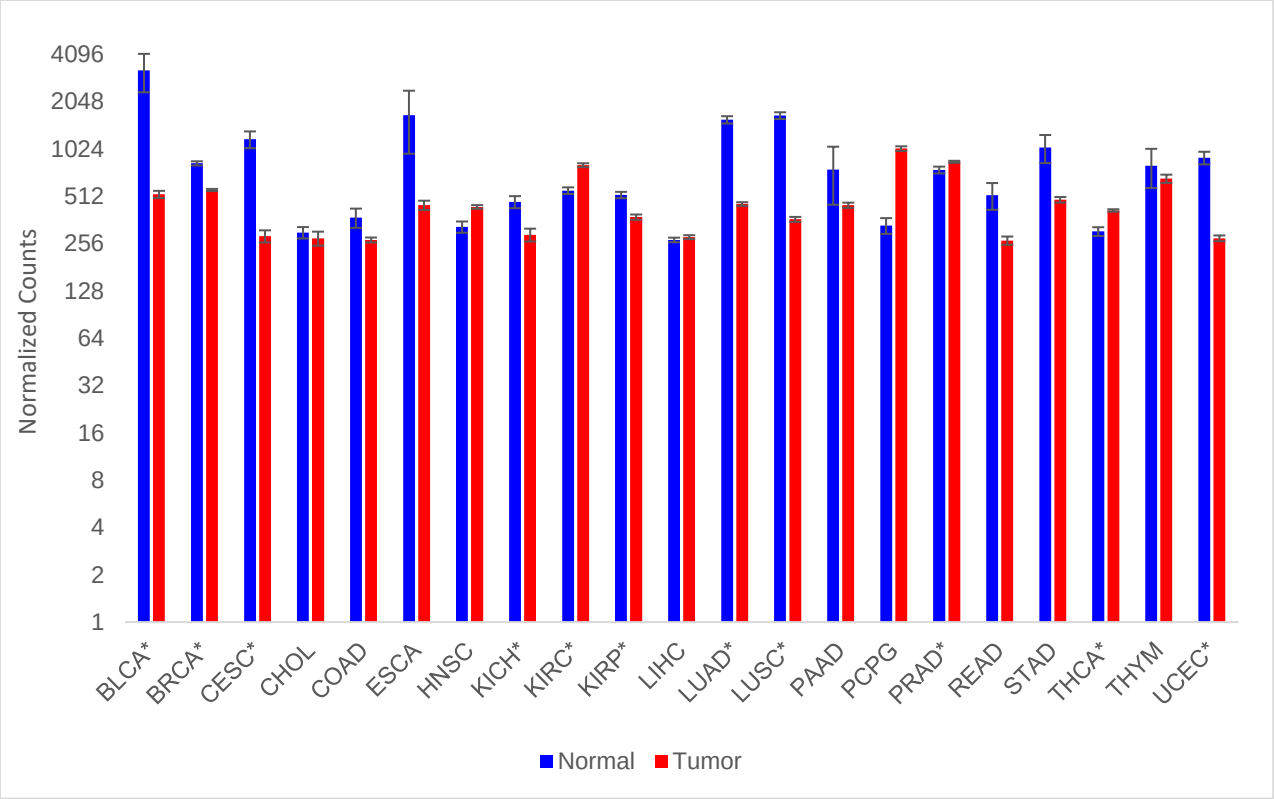

Supplementary Figure S13: ADARB1 (ADAR2) expression in human cancers. RSEM normalized counts are shown for each tissue type. *p<0.05 Mann-Whitney test followed by a Benjamini Hochberg multiple testing correction. Error bars denote ±SEM. See Supplementary Table S1 for tissues acronyms.